Flow interaction of diffuser augmented wind turbines

U Göltenbott[1], Y Ohya[2], S Yoshida[2] and P Jamieson[3]

[1] Department of Aeronautics and Astronautics, Kyushu University, 744 Motooka, Nishi-ku, Fukuoka 819-0395, Japan
[2] Research Institute for Applied Mechanics, Kyushu University, 6-1 Kasuga-koen, Kasuga 816-8580, Japan
[3] Wind Energy DCT, University of Strathclyde, Royal Collage R336, Glasgow, G1 1XW, Scotland

E-mail: uli@riam.kyushu-u.ac.jp

Abstract. Up-scaling of wind turbines has been a major trend in order to reduce the cost of energy generation from the wind. Recent studies however show that for a given technology, the cost always rises with upscaling, notably due to the increased mass of the system. To reach capacities beyond 10 MW, multi-rotor systems (MRS) have promising advantages. On the other hand, diffuser augmented wind turbines (DAWTs) can significantly increase the performance of the rotor. Up to now, diffuser augmentation has only been applied to single small wind turbines. In the present research, DAWTs are used in a multi-rotor system. In wind tunnel experiments, the aerodynamics of two and three DAWTs, spaced in close vicinity in the same plane normal to a uniform flow, have been analysed. Power increases of up to 5% and 9% for the two and three rotor configurations are respectively achieved in comparison to a stand-alone turbine. The physical dynamics of the flows are analysed on the basis of the results obtained with a stand-alone turbine.

1. Introduction

A major trend in the wind turbine industry is increasing the size of the rotor in order to generate more energy and to reduce the cost of energy generated from the wind. This was notably possible due to technological advancements in fiber reinforcements to manufacture longer blades. Currently, researchers focus on developing technologies to scale wind turbines to 10 MW and beyond. However, there are certain issues related to the upscaling of wind turbines which have been discussed by Jamieson and Branney [1] and Sieros et al. [2] who stated that upscaling usually results in an unfavorable weight increase for a given technology level. On the other hand, Hofmann and Sperstad [3] pointed out that low failure rates and short maintenance durations are crucial to achieve low cost of energy. A concept to overcome these issues for wind turbines is the multi-rotor system (MRS), defined as containing more than one rotor in a single structure. Upscaling the rotor swept area by increasing the number of rotors instead of the diameter of a single rotor leads to significant savings in mass. The additional structural mass to hold multiple rotors in place doesn't outweigh the mass saving, therefore providing a high potential to reduce the levelised cost of energy [1].

The concept of multi-rotor systems has been around for over 100 years [4-7]. In the last decade, seven rotor systems have been analyzed experimentally [8] and using CFD [9] and found no negative interferences between rotors. On a larger scale, structural considerations of a 20 MW multi-rotor

system with 45 rotors have been presented by Jamieson and Branney [1]. They showed that mass and cost are reduced, in comparison to a single rotor turbine with the same power, and that the structure is designed based on the aerodynamic forces rather than on the rotor loading.

Innovations to increase the performance of wind turbines have led to the use of ducts around the rotor to augment the flow. There has been extensive experimental analysis performed by many researchers over the past 50 years [10-13]. Research in diffuser augmented wind turbines (DAWTs) is still ongoing [14, 15]. Although performance up to 2 to 5 fold has been achieved in wind tunnel experiments [16], there are structural challenges in upscaling diffusers to be used with large wind turbines.

In the work presented in this paper, DAWTs are used in a multi-rotor configuration. To make use of the increased performance of a DAWT, the integration into a multi-rotor system is promising.

Research presented by Wang and Chen [17] analyzed two DAWTs, which yawed individually with wind from different angles. They have placed turbines with gaps of ***s/D*** of 0.22, 0.44 and 0.67, where ***s*** is gap widths and ***D*** is the external diameter. The focus of the study was to investigate the deficit of a DAWT in the wake of a turbine upstream at different wind directions. Although not discussed in the paper, the graphs show a small increase in power, in the order of 2 - 5%, when the DAWTs are set normal to the inflow. Ohya et al. [18] conducted experiments with three brimmed DAWTs in a MRS measuring both drag coefficients and power coefficients simultaneously. Drag and power coefficients correlated very well.

In wind tunnel experiments presented in this paper, the effects of spacing of brimmed DAWTs with various shroud diameters on their aerodynamic performance are analyzed. The brim, which is attached to the DAWTs, is the crucial feature because it is responsible for the vortex shedding. The turbines are set in the same plane, next to each other, without the ability to yaw individually since a multi-rotor system is meant to yaw as a whole. Up to three turbines are placed side-by-side to measure power coefficients. The average power coefficient of a multi-rotor configuration is compared with a single, stand-alone turbine. The analysis has been carried out for multi-rotor systems using conventional turbines and DAWTs. To explain the results, similarities with the phenomena observed in the flow around multiple bluff bodies and vortex shedding from three dimensional bodies are drawn.

2. Experimental Setup

The wind turbines are placed in the wind tunnel test section, which has a cross section of 3.6 m by 2 m and a length of 15 m. An outline of the boundary layer wind tunnel can be seen in Figure 1.

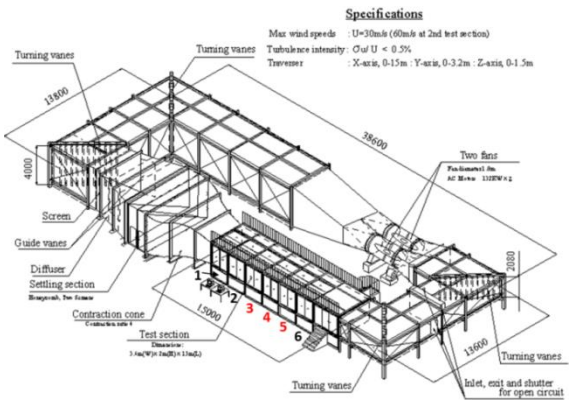

Figure 1. Wind tunnel specifications with side walls and ceiling plates removed for elements number 3, 4 and 5 [19].

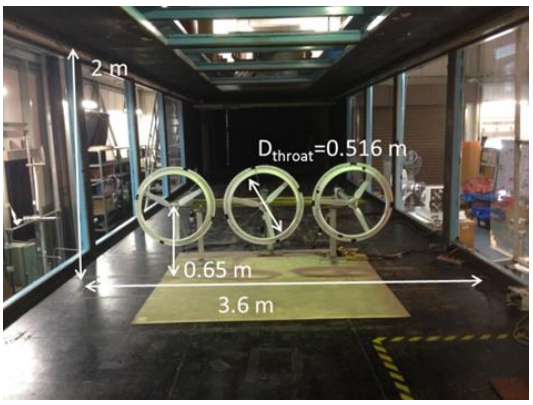

Figure 2. Turbine setup in the wind tunnel, with view in the flow direction showing the three DAWTs configuration.

The test section consists of 6 elements, where the side walls and ceiling plates have been removed for the elements number 3, 4 and 5. With the removal of the side walls and ceiling plates, the wind tunnel becomes semi-open, which significantly decreases blockage effects.

The rotor plane of the turbines is positioned 1 m downstream from the first opened side walls. Configurations of two turbines and three turbines, placed side-by-side normal to the uniform flow, are analyzed. The setup for the three DAWT configuration can be seen in Figure 2. The rotor shafts of the turbines are located 0.65 m above the floor, which leaves a distance of approximately 0.31 m between the brim and the floor. Horizontally, the turbines are aligned with the center of the wind tunnel. The minimum distance to the side wall is 0.4 m. The effect of the vicinity of the turbines to the side walls, floor and ceiling on the results has been tested and showed negligible small variations.

The shape of the diffusers, with the shroud attachments, can be seen in Figure 3. All diffusers used in this study have the same diffuser shape denoted as Ci-Diffuser. The depth of the Ci-Diffuser is 0.137 throat diameter $\boldsymbol{D_{throat}}$, defined as the inside diameter of the diffuser, and follows a cycloid curve. The shrouded brims have heights from 0.03 to 0.1 throat diameters (3 – 10%). The denotation used is B03 for 3%, B05 for 5%, B07 for 7% and B10 for 10%, respectively [16].

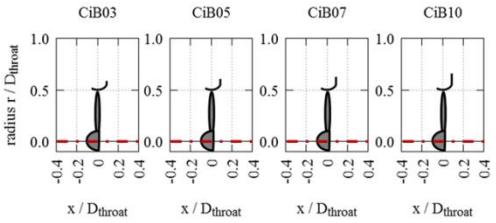

Figure 3. Duct shape normalized to throat diameter, $\boldsymbol{D_{throat}}$ for Ci-Diffuser with brim heights from 3 to 10%.

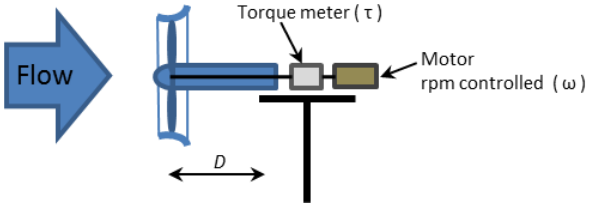

Figure 4. Measurement setup.

2.1. Power measurements

The rotors are driven by a motor using a torque meter as a link between the rotor shaft and the motor shaft, as shown in Figure 4. The rotational speed **ω** is set constant and torque **τ** is measured with the signal fed into the PC through an AD-Converter. Sampling time for **τ** is 20 seconds at a sampling frequency of 100 Hz. Measurement error is estimated to be in the order of ± 0.5%.

To adjust the gap, the turbines are moved horizontally on a rail. Approximately 1 ***D*** downstream, where ***D*** is the external diameter of the brim of one turbine, a torque meter is connected to the rotor shaft. On the other end of the torque meter, a speed-controlled motor is connected. Assuming constant inflow velocity, the optimum tip speed ratio is realized by setting a constant rotational speed of the rotor. For the period of measurement, the motor speed is held constant by the motor controller. The two turbine configuration, with a description of the main dimensions, is illustrated in Figure 5.

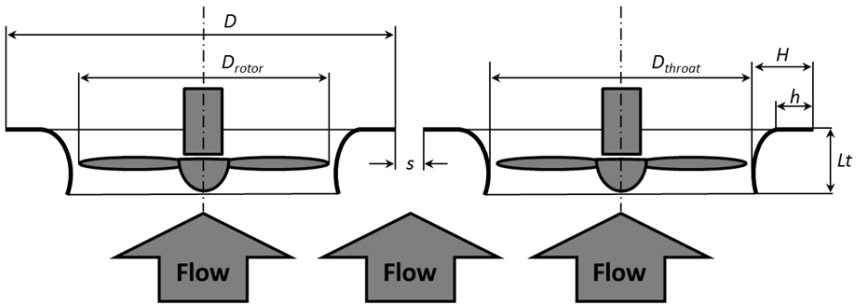

Figure 5. Schematics of two brimmed DAWTs placed side-by-side.

The rotor blades, produced with a 3D-printer, have cross-sections of MEL-type aerofoils [20]. At a wind speed of 7 m/s, the Reynolds numbers ***Re***, using the brim diameter of the DAWTs as characteristic length ***L***, are shown in Table 1. For the conventional turbine, ***D*** is equal to the rotor

diameter. Reynolds number regarding the blade is the chord length of the blade as the characteristic length. The Reynolds number is obtained using:

$$Re = \frac{U_0 \cdot L}{\nu} \quad (1)$$

with U_0 = wind speed of the approaching flow in the wind tunnel, L = characteristic length and ν = kinematic viscosity of the air at the ambient temperature of the experiment. The rotation direction of the rotors is clockwise for all turbines, as seen in the flow direction.

Table 1. Characteristic length ***L*** and corresponding Reynolds numbers ***Re***.

	Conventional	CiB03	CiB05	CiB07	CiB10	Blade (***L***=chord length)
***L* = *D* [m]**	0.512	0.595	0.615	0.636	0.667	0.06
Re **$\times 10^5$**	2.37	2.76	2.85	2.95	3.09	0.28

3. Bluff body flow

Studying the flow around bluff bodies has been very useful to understand the basic flow phenomena. Relevant to the flow around multiple rotors surrounded by shrouded diffusers, two bluff body flow phenomena are reviewed. Firstly, the flow around multiple bluff bodies is discussed for flat plates and circular cylinders. Secondly, the behaviour of vortex shedding from a square prism is explained. These flow phenomena and their applications to wind turbines have been summarized in detail by Ohya [21].

3.1. Flow around multiple bodies

The flow through the gap of a pair of flat plates arranged side-by-side showed that biasing of the gap flow in the near wake influences the drag coefficients of each plate [22]. The flat plate on the side of which the flow is biased shows higher drag and regular vortex shedding, where the plate on the other side shows the opposite. The bi-stable flow patterns occurred in a stable manner for a certain time period until it changed to the other pattern. The biased gap flow was observed for gap ratios ***s/D*** < 2, where s is the gap width and ***D*** is the body width.

A pair of circular cylinders also show biased gap flow patterns in a similar way as the pair of flat plates. The gap ratios where biased gap flows appear are also similar to the ones observed using flat plates. However, the flow patterns using cylinders shifted randomly at irregular intervals [22].

Table 2. Ratio of gap ***s*** to projected width of the duct ***H***, ***s/H*** as a function of the gap ratio ***s/D*** for the configurations studied.

		s/D						
		0	0.05	0.1	0.15	0.2	0.3	0.5
s/H	CiB03	0.00	0.75	1.51	2.26	3.01	4.52	7.53
	CiB05	0.00	0.62	1.24	1.86	2.48	3.73	6.21
	CiB07	0.00	0.53	1.06	1.59	2.12	3.18	5.30
	CiB10	0.00	0.44	0.88	1.33	1.77	2.65	4.42

A DAWT with air flowing through the rotor can be regarded as a solid ring structure with free flow around the outside and restricted flow through the inside where the rotor is located. Assuming the DAWT acts as a circular flat disc, the body width is the brim diameter ***D*** and the gap ratio becomes ***s/D***. With air passing through the inside of the duct, the projected widths of the ring structure ***H*** can be regarded as a second parameter for the gap ratio ***s/H***. In Table 2, the gap ratios ***s/D*** and ***s/H*** are shown for each experimental setup with each diffuser-brim configuration.

3.2. Vortex shedding from three dimensional bodies

Nakamura and Ohya [23] used two hot wires to estimate the vortex shedding frequency on two sides of a square prism. They found that the vortex shedding occurs either in one or the other plane. However, the vortex shedding around the circular brim of a DAWT appears to be random [21]. With the introduction of so-called vortex control plates, the shedding around the circular circumference of the brim can be organized and strengthened in each segment, resulting in small increases in performance, as reported by Ohya [21].

When placing two turbines side-by-side, the general appearance of the setup can be seen as one body being much wider than its height. Therefore, vortex shedding is likely to happen in the plane of the shorter distance. In a side-by-side configuration of two or three DAWTs, the shedding preferably occurs over the edges of the brim facing the top and the bottom.

4. Measurement procedure for turbine power output

First, the power coefficient of each stand-alone turbine is measured one-by-one. The power coefficient for this single turbine configuration, C_{P0i}, is calculated as:

$$C_{P0i} = \frac{P_{Turbine}}{P_{Wind}} = \frac{\tau \cdot \omega}{\frac{1}{2}\rho A U_0^{\,3}} \qquad (2)$$

with the power in the wind, P_{Wind}, calculated with the air density ρ, the wind speed U_0 and the area, A swept by the rotor. The rotor swept area is used as a reference for both the conventional turbine and the DAWT. For its part, the power from the turbines, $P_{Turbine}$, is calculated from the torque τ measured by the torque meter and the angular velocity ω of the rotor (Figure 4). Figure 6 shows the power curves, as a function of the tip speed ratio λ, of a conventional turbine and DAWTs using a Ci-Diffuser with brim heights ranging from B03 to B10. At λ= 4.2, the DAWT with B10 shows an irregularity which is assumed to be a measurement error that originates from a resonance frequency of that rotational speed of the rotor. Therefore, the wind speed U_0 was chosen to make sure that the peak of maximum power coefficient is not affected by errors from resonance frequencies. The results clearly show that the performances of the DAWTs are significantly above the conventional turbine. Within the diffuser augmented turbines, the best performance is achieved with brim heights between 5% and 10%, where the brim heights are referenced to the throat diameter, D_{throat} .

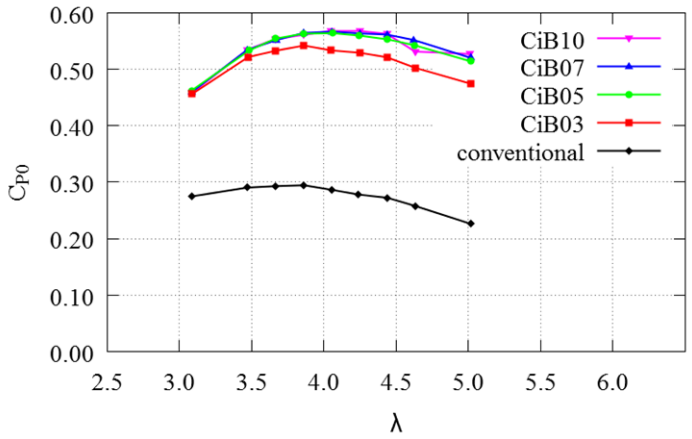

Figure 6. Power coefficients as a function of the tip speed ratio, of a stand-alone conventional turbine and DAWTs.

The maximum power coefficient, $C_{P0i\text{-}max}$ of each turbine in stand-alone configuration is measured at their optimum tip speed ratio. The average of these maximum power coefficients of all n turbines in stand-alone configuration is defined as:

$$\overline{C_{P0-\max}} = \frac{C_{P01-\max} + \cdots + C_{P0n-\max}}{n} \tag{3}$$

After that, the power coefficients of the wind turbines in two and three turbine configurations are measured simultaneously. In the multi-rotor configuration, the power coefficient is denoted as $C_{Pi\text{-}max}$ for each turbine. The average power coefficient of the MRS containing n turbines is then defined as:

$$\overline{C_{P-\max}} = \frac{C_{P1-\max} + \cdots + C_{Pn-\max}}{n} \tag{4}$$

To understand how the power coefficient changed in each turbine, the $C_{Pi\text{-}max}$ from each turbine in the MRS configuration is compared to the $C_{P0i\text{-}max}$ of each in the stand-alone configuration. Therefore, the variation, $Var\_C_{Pi\text{-}max}$ is defined as:

$$Var\_C_{Pi-\max} = \left(\frac{C_{Pi-\max}}{C_{P0i-\max}} - 1 \right) \tag{5}$$

In order to compare the average power coefficient of the MRS with the average power coefficient of the stand-alone wind turbines, the variation, $Var\_C_{P\text{-}max}$ is defined as:

$$Var\_C_{P-\max} = \left(\frac{\overline{C_{P-\max}}}{\overline{C_{P0-\max}}} - 1 \right) \tag{6}$$

In the MRS configuration $Var\_C_{P\text{-}max}$ is estimated for each gap ratio s/D from 0 to 0.5 for the two turbines MRS and 0.2/0.3 for the three turbines MRS. It should be mentioned that the optimum tip speed ratio didn't change significantly when clustering the wind turbines in a MRS.

5. Performance of multiple turbines

The performance of multiple turbines in an array was evaluated by placing two, and later three turbines, side-by-side and by measuring the power output in the wind tunnel.

5.1. Total power output of turbines

First, two turbines were placed side-by-side and the power output was measured and compared to each stand-alone turbine. The smallest gap for the two conventional turbines was chosen to be 2.5% of the rotor diameter, mimicking a safety gap to avoid collision of the rotor blades. The turbines show a power increase of around 1% for all the gap ratios ranging between 0.025 and 0.5 of the external diameter D which, in the case of the conventional turbine, is the rotor diameter D_{Rotor}, seen in Figure 7. For their parts, at $s/D = 0$, the DAWTs only exhibit small increases in power. In this setup, the brims of neighbouring turbines are in direct contact. When further increasing the gap between turbines, the power increases to a maximum of 3% for CiB03 and 5% for CiB10, seen in Figure 7.

Next, the power coefficients of three turbines side-by-side are measured at various gaps. Figure 8 shows that the conventional turbine's increase in total power output is between 3 and 5%. The source of oscillation of the measured C_P is yet unknown; it could come from rotor wake interference. For the DAWTs, an increase at 0 D gap starting from 2% with CiB05 to almost 5% with CiB10 was observed. The peak of power increase was reached at a gap of 0.15 D in most cases. Maximum power increase reached 4.5% for the conventional turbines and 9% for the DAWT using the CiB10 configuration. The three turbine configuration was measured until a gap ratio of $s/D = 0.2$ and 0.3, allowing to stay well inside the test section of the wind tunnel. If and how much the C_P will continue to increase is unknown.

In an experiment with smaller turbines, we observed that interferences beyond a gap ratio of ***s/D*** = 1 diminish and consequently C_P drops back to the stand-alone values.

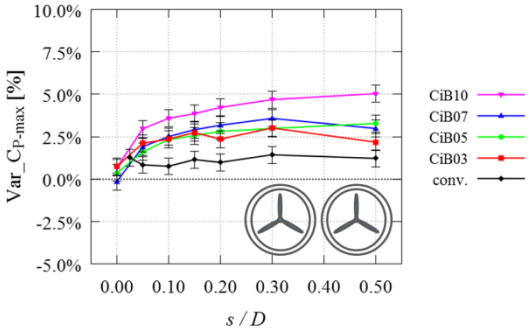

Figure 7. Power variation as a function of the gap between two turbines side-by-side.

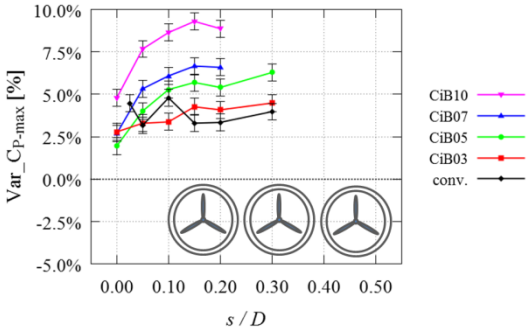

Figure 8. Power variation as a function of the gap between three turbines side-by-side.

5.2. Individual turbine power output

For the three turbine configuration, when looking at the power output of each individual turbine in the MRS, there are cases where a turbine is not equally contributing to the trend of the average power output of the three turbine MRS. Figure 9 shows the increase in power output of the three DAWTs in the CiB05 configuration. The power increase for turbines on the left, middle and right side is shown with the total power increase. It can be observed that the turbine on the left side shows very similar power increase as the total power increase. The turbine in the middle shows higher increases and the turbine on the right side shows lower increases than the total. Figure 10 shows the increase in the power output of the three DAWTs in the CiB10 configuration, where the difference in power output is rather negligible.

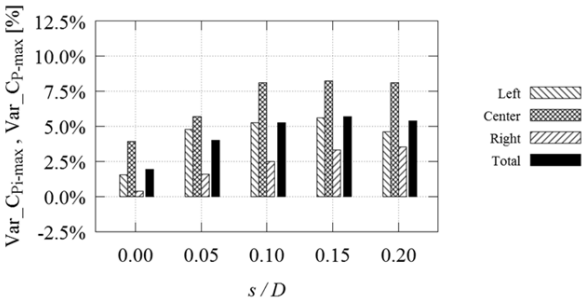

Figure 9. Individual turbine power variation with three DAWTs in the CiB05 configuration.

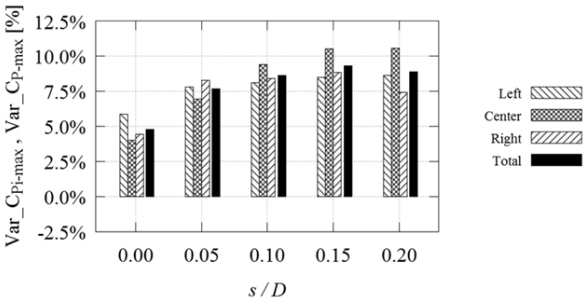

Figure 10. Individual turbine power variation with three DAWTs in the CiB10 configuration.

6. Discussion

The experimental results show that the configurations of up to three conventional turbines do not exhibit significant interference regarding the power output. These findings confirm what has previously been reported for conventional turbines with narrow gaps [7, 8].

Using DAWTs in two or three turbine MRS configurations showed increased power output which depends on the gap ratio. The maximum increase in total power output from two DAWTs was between 3 and 5%. For three DAWTs, the maximum total power increase was between 5 and 9%.

One of the aerodynamic mechanisms of the DAWT is the vortex shedding from the brim that reduces the back pressure and therefore increases the power output of the turbine. When turbines are placed next to each other with the brims in direct contact, the vortex shedding is inhibited at that point, which would result in the decreased power output. However, small power increases were observed for

both two and three turbine configurations. As reported by Ohya [21], vortex shedding around a single turbine occurs in a random manner around the circumference of the brim. Research by Nakamura and Ohya [23] showed that vortex shedding prefers to occur in one plane. Two DAWTs placed directly in contact side-by-side appear as one object being at least twice as wide as it is high. Therefore, vortex shedding could be strengthened over the shorter plane, thus maintaining or even decreasing the back pressure which leads to the power increase.

For gap ratios s/D larger than 0, air can pass through the gap. Hence, vortex shedding becomes possible around the whole circumference of the brim edge of each turbine's brim, which contributes to higher power output of the MRS using DAWTs.

When looking at each turbine in the MRS, it was found that sometimes each turbine showed rather different power increases. At gap ratios of s/D = 0.1 and 0.15, the three DAWTs with CiB05 configuration seen in Figure 9 show that the power increase of the centre turbine is significantly higher than the power increase of the turbines on the sides. From research about the gap flow between bluff bodies as described in section 3.1, it was learned that there are interactions between vortices that can lead to a biased gap flow [22]. A biased gap flow is characterized by a change in flow direction behind the gap. If stable for a certain period of time, contrary drag forces were measured at neighbouring bodies. Several flow patterns are possible, each being bi-stable and therefore a change in pattern is possible at random intervals [22]. From the experiments by Ohya et al. [18] biased gap flow was measured with a hot wire probe behind two circular discs placed side-by-side with small gaps. It was shown that the drag coefficient of each disc is affected by the biased gap flow. The disc on the biased side of the flow shows higher drag and the disc on the other side shows lower drag. With the correlation of the increase in drag and power coefficients of DAWTs it can be assumed that differences in power coefficients of DAWTs in a multi-rotor configuration are affected by gap flow patterns. Therefore, the drag coefficient was not measured in this study.

Depending on the gap flow pattern present at the time, the power coefficient of each of the three turbines can show differing values similar to the drag forces of bluff bodies. In the case presented in Figure 9 using CiB05 at gap ratios s/D = 0.1 and 0.15, the gap flow pattern seems to be unbiased between the left and the centre turbines. Between the centre and right turbines, the gap flow seems to be biased towards the centre turbine, which explains why the power output of the turbines is not symmetric. The results from the three turbine configuration using CiB10 seen in Figure 10 don't show significant differences in power increase between each turbine. The gap flow seems to be unbiased in the gaps between all three turbines, which results in a rather symmetric and evenly distributed increase in power output of the turbines.

In an attempt to visualize the biased gap flow, a smoke wire technique was used in the CiB05 and CiB10 configurations. In order to get clear smoke lines, a wind speed of U_0 = 3 m/s was used, which results in a Reynolds number of less than half of the one used in the power measurements. With such a low Reynolds number, the flow around the aerofoils of the blades is not as well established, which resulted in unsuitable power measurements. Observations showed small biasing which randomly shifted direction in irregular time intervals. It wasn't possible to see a stable flow pattern that could be linked to the differences in power output, which were measured at higher Reynolds numbers.

Vibrations induced into the structure due to vortex shedding from the brims of the DAWTs have not been observed in the experiments at the given Reynolds number. The reason for this is that the vortex shedding occurs randomly around the circumference of the brims of the DAWTs.

7. Conclusion

In the wind tunnel experiments, the aerodynamics of two and three brimmed DAWTs spaced in close vicinity in the same plane normal to a uniform flow have been analysed. For gap ratios s/D between 0 and 0.5, conventional turbines and DAWTs showed an increase in power output. DAWTs show higher power increases than conventional turbines, reaching its maximum of 9% at around s/D = 0.15 gap between neighbouring brims. The power increase is further dependent on the brim height of the diffuser. The highest power increase was observed with a 10% brim height (CiB10). It can thus be

concluded that DAWTs installed in side-by-side configurations, with suitable spacing and appropriate brim heights, increase the efficiency of the same wind turbines taken individually.

In some cases, each DAWT in a MRS, showed differences compared to the average power output of the whole MRS. With phenomena from bluff body flows, these differences can be explained. From the flow around multiple bodies, biased gap flows were observed that affected the drag coefficients of each bluff body and the average of the bluff bodies. Similarities between the drag coefficients of bluff bodies and power coefficients of DAWTs have been shown [18].

Using a smoke wire technique to visualize the gap flow at low wind speeds didn't show any distinctive patterns. The flow around square prisms has shown that vortex shedding prefers to occur at opposite edges of the prism. This means that vortex shedding prefers to occur in one or the other plane, but not in both planes at the same time. In a two or three turbine MRS, the DAWTs appear as one object with a width of two or three times the height. Due to the two dimensional appearance of the MRS vortex shedding could be strengthened with lower back pressure, leading to increased rotor performance. This can be seen as the reason why the power of DAWTs in direct contact still show an increase in power output.

In this study the power coefficient of DAWTs has been calculated in relation to the rotor swept area. Using the outer diameter of the brim instead of the rotor swept area, the power coefficient of DAWTs is still above the power coefficient of a conventional wind turbine. It is yet to be examined how the performance is affect for MRS with more than three DAWTs. Furthermore, it must be clarified if the aerodynamic performance outweighs the additional cost for the brimmed diffuser in a MRS with DAWTs.

It can be concluded that brimmed DAWTs in MRS show very interesting flow interactions. These can lead to an increase in power output compared to a single DAWT. Future work includes analysing the interactions by adding more DAWTs, while CFD simulations would provide more details on the flow field, notably in regards to the gap flow between the turbines.

8. Acknowledgment

Acknowledgments go to Mr. Kimihiko Watanabe and Mr. Keiji Matsushima for their contributions in the wind tunnel experiments. Further, the Ministry of Education, Culture, Sports and Science (MEXT) of Japan is acknowledged for the scholarship support for the first author.

References

[1] Jamieson P and Branney M. Multi-Rotors; A Solution to 20 MW and Beyond? Energy Procedia 2012; 24: 52-59.
[2] Sieros G, Chaviaropoulos P, Sørensen JD, Bulder BH and Jamieson P. Upscaling wind turbines: theoretical and practical aspects and their impact on the cost of energy. Wind Energy 2012; 15: 3-17.
[3] Hofmann M and Sperstad IB. Will 10 MW Wind Turbines Bring Down the Operation and Maintenance Cost of Offshore Wind Farms? Energy Procedia 2014; 53: 231-238.
[4] Nielsen JV. Danmarks Vindkrafthistoriske Samling (Danish Wind Historical Collection). URL: http://www.vindhistorie.dk/userfiles/downloads/faktablade/Faktablad_2a.pdf. accessed on 31.05.2016
[5] Jamieson, P. Innovation in Wind Turbine Design, John Wiley & Sons, Ltd, 2011.
[6] Heronemus W. Pollution-free energy from offshore winds. 8th Annual Conference and Exposition, Marine Technology Society, Washington, DC 1972.
[7] Smulders PT, Orbons S and Moes C. Aerodynamic interaction of two rotors set next to each other in one plane. European Wind Energy Conference, Hamburg 1984; 529-533.
[8] Ransom D, Moore JJ and Heronemus-Plate M. Performance of wind turbines in a closely spaced array. Renewable Energy World 2010; 2 32.

[9] Chasapogiannis P, Prospathopoulos JM, Voutsinas SG and Chaviaropoulos TK. Analysis of the aerodynamic performance of the multi-rotor concept. Journal of Physics: Conference Series 2014; 524: 012084.
[10] Rainbird WJ, Lilley GM. A preliminary report on the design and performance of a ducted windmill [Report 102]. College of Aeronautics Cranfield. 1956.
[11] Foreman K, Gilbert B and Oman R. Diffuser augmentation of wind turbines. Solar Energy 1978; 20: 305-311.
[12] Igra O. Research and development for shrouded wind turbines. Energy Conversion and Management 1981; 21: 13-48.
[13] Abe K, Nishida M, Sakurai A, Ohya Y, Kihara H, Wada E and Sato K. Experimental and numerical investigations of flow fields behind a small wind turbine with a flanged diffuser. Journal of Wind Engineering and Industrial Aerodynamics 2005; 93: 951-970.
[14] van Bussel GJW. The science of making more torque from wind: Diffuser experiments and theory revisited. Journal of Physics: Conference Series 2007; 75: 012010.
[15] Hansen MOL, Sørensen NN and Flay RGJ. Effect of Placing a Diffuser around a Wind Turbine. Wind Energy 2000; 3: 207-213.
[16] Ohya Y and Karasudani T. A Shrouded Wind Turbine Generating High Output Power with Wind-lens Technology. Energies 2010; 3: 634.
[17] Wang SH and Chen SH. The Study of Interference Effect for Cascaded Diffuser Augmented Wind Turbines. The 7th Asia-Pacific Conf. on Wind Eng. Taipei, Taiwan. 2009; 8-12.
[18] Ohya Y, Miyazaki J, Göltenbott U, Karasudani T, Yoshida S. Power augmentation of shrouded wind turbines in a multi-rotor system. Proceedings of 2nd International Conference On Next Generation Wind Energy (2nd ICNGWE), Lund, Sweden, August 24-26, 2016.
[19] Boundary Layer Wind Tunnel, Wind Engineering Section, Research Institute for Applied Mechanics, Kyushu University. URL: http://www.riam.kyushu-u.ac.jp/windeng/equipment.html accessed on 06.07.2016
[20] Matumiya T, Kogaki T, Iida M and Kieda K. A development of high performance aerofoil. Turbomachinery 2001; 29: 519-524
[21] Ohya Y. Bluff body flow and vortex—its application to wind turbines. Fluid Dynamics Research 2014; 46: 061423.
[22] Ohya, Y, Okajima, A, and Hayashi, M. Wake Interference and Vortex Shedding. Encyclopedia of Fluid Mechanics (ed. N.P. Cheremisinoff), Gulf Publishing Corporation, Houston 1989; 323–389.
[23] Nakamura Y and Ohya Y. Vortex shedding from square prisms in smooth and turbulent flows. J. Fluid Mech. 1986; 164: 77-89.